Available online at www.sciencedirect.com
ScienceDirect
Computerized Medical Imaging and Graphics 31 (2007) 28–38
Computerized Medical Imaging and Graphics
www.elsevier.com/locate/compmedimag

Quantitative analysis of template-based attenuation compensation in 3D brain PET

Marie-Louise Montandon, Habib Zaidi *

Division of Nuclear Medicine, Geneva University Hospital, CH-1211 Geneva 4, Switzerland

Received 3 November 2005; accepted 28 September 2006

Abstract

An atlas-guided attenuation correction method was recently proposed for 3D brain positron emission tomography (PET) imaging eliminating the need for acquisition of a patient-specific measured transmission scan. The algorithm was validated through comparison to transmission-based attenuation correction (gold standard) using voxelwise statistical parametric mapping (SPM) analysis of clinical data. In contrast to brain 'activation' studies for which SPM is primarily developed, brain PET research studies often involve absolute quantification. In the preliminary validation study published earlier, there is no validation as to how such quantification can be affected by the two methods as the assessment was carried out by an SPM group analysis alone. It is quite important to demonstrate how the proposed method performs individually, particularly for diagnostic applications or individual quantification. In this study, we assess the quantitative accuracy of this method in clinical setting using automated volume of interest (VOI)-based analysis by means of the commercially available *BRASS* software.

There is a very good correlation ($R^2 = 0.91$) between the atlas-guided and measured transmission-guided attenuation correction techniques and the regression line agreed well with the line of identity (slope = 0.96) for the grouped analysis of patient data. The mean relative difference between the two methods for all VOIs across the whole population is 2.3% whereas the maximum difference is less than 7%. No proof of statistically significant differences could be verified for all regions. These encouraging results provide further confidence in the adequacy of the proposed approach demonstrating its performance particularly for research studies or diagnostic applications involving quantification.

Keywords: PET; Attenuation correction; Brain imaging; Template; Quantitative analysis

1. Introduction

The specific role of positron emission tomography (PET) imaging in the expansion of our understanding of the pathophysiological mechanisms of neurological and psychiatric diseases and in the clinical management of patients is steadily progressing [1–3]. During the last two decades, non-invasive three-dimensional (3D) molecular mapping of brain function with PET has improved markedly through the development of dedicated instrumentation and the synthesis of new radiopharmaceuticals [4]. Quantification of brain function using PET is promising and remains an active research topic [5]. PET offers the possibility of truly quantitative (physiological) measurements of tracer concentration *in vivo*. However, there are several issues that must be considered in order to fully realize this potential [6]. It is well accepted that photon attenuation in tissues is the primary physical degrading factor limiting both visual qualitative interpretation and quantitative analysis capabilities of reconstructed PET images [7,8]. Measured transmission-based attenuation correction in cerebral 3D PET imaging is the most commonly used procedure both in clinical and research settings since it is expected to yield the best attenuation map as a result of matched energy and spatial resolution [9]. However, motion-induced misalignment between transmission and emission scans can result in erroneous estimation of regional tissue activity concentrations [10]. It is recognized that misregistration of PET and transmission images can be minimized through post-injection transmission scanning protocols; however, spillover of emission data into the transmission energy window remains a major problem of this technique. The most commonly used approach to eliminate or reduce this source of errors and artefacts estimates the emission contamination of the post-injection scan using a short transmission "mock" scan performed after tracer administration, which again increases the acquisition time and patient motion is still present. Likewise, the high cost of combined PET/CT units and the potential introduction of

* Corresponding author. Tel.: +41 22 372 7258; fax: +41 22 372 7169.
E-mail address: habib.zaidi@hcuge.ch (H. Zaidi).

0895-6111/$ – see front matter © 2006 Elsevier Ltd. All rights reserved.
doi:10.1016/j.compmedimag.2006.09.017

artefacts in case of misregistration of PET and CT images, errors in the calibration procedures [11], contribution of X-ray scatter in CT images and administration of oral or intravenous contrast medium [12], and the presence of metallic dental implants [13] or EEG electrodes for epilepsy patients when using CT-based attenuation correction, thus biasing quantitative PET estimates and disturbing the visual interpretation of PET images are major limitations for brain imaging dedicated facilities.

The need of acquiring an additional transmission scan complicates the scanner design and is a restrictive factor since it represents a substantial increase in the overall acquisition time, thus decreasing patient comfort and scanner throughput. In most protocols used in clinical PET facilities, the transmission scanning time accounts for over 30% of the total acquisition time. The search for reduction of acquisition time in brain PET scanning protocols spurred the development of transmissionless algorithms for derivation of the non-uniform attenuation map, thus eliminating the need for acquisition of a measured transmission scan [14–17]. More recently, we investigated the implementation and applicability of atlas-guided attenuation correction [18]. Twelve cerebral clinical studies were used for evaluation of the developed attenuation correction technique as compared to the standard pre-injection measured transmission-based method used in clinical routine (gold standard). The subjective qualitative assessment showed no significant visual differences between atlas-guided and transmission-based attenuation correction methods. However, the quantitative voxel-based analysis using statistical parametric mapping (SPM2) [19] comparing atlas-guided to transmission-based attenuation corrections suggested that regional brain metabolic activity increases significantly bilaterally in the superior frontal and precentral gyri, in addition to the left middle temporal gyrus and the left frontal lobe. Conversely, activity decreases in the corpus callosum in the left parasagittal region.

It was hypothesized that the overall diagnostic accuracy may not be too influenced by application of either of the two correction methods for certain diseases such as dementia of Alzheimer's type (DAT), but regional quantitative accuracy is most likely affected. If regional discrepancies are not anatomically consistent (i.e., differences in regional attenuation between atlas estimates and actual individual brains), the SPM group validation alone is not sufficient to depict effects and limitations of the proposed attenuation correction method. It is quite important to demonstrate how the proposed method performs individually, particularly for diagnostic applications or individual quantification. In this paper, we further assess the quantitative accuracy of this method in clinical setting using volume of interest (VOIs)-based analysis by means of the commercially available *BRASS* program for automatic fitting and quantification of functional brain images [20].

2. Materials and methods

2.1. Atlas-guided attenuation correction

The proposed algorithm derives a patient-specific attenuation map by anatomic standardization through non-linear warping of a stereotactic transmission template obtained by averaging 11 scans of normal subjects [18]. This transmission template is coregistered to a specially designed tracer-specific ^{18}F-[FDG] emission template constructed by scanning 17 normal subjects in resting condition during tracer uptake in a dark room [21]. The emission template is first coregistered and spatially normalized to preliminary PET images of subjects corrected for scatter and attenuation using an approximate method since this has been shown to improve registration accuracy. The preliminary 3D PET reconstructions relied on calculated attenuation correction, which was performed by approximating the outline of the head on each transverse slice using a manually drawn slice-dependent ellipse assuming uniform attenuation ($\mu = 0.096\,\mathrm{cm}^{-1}$) for brain tissues. The main drawbacks of this technique are the time required to draw each ROI, operator dependence of the results and bias caused by the fact that the head is not perfectly elliptical, nor does it have uniform density. The resulting transformation matrices are recorded and re-applied to the transmission template. The attenuation of the rigid bed made of carbon fibre was neglected but could be readily incorporated in the algorithm by addition of a good statistics bed image after adjustments to account for different bed elevations [22]. The derived attenuation map is then forward projected to generate attenuation correction factors to be used for correcting the subjects' PET data. Fig. 1 shows a diagram describing the general principles of the method and main steps required to generate a patient-specific attenuation map.

2.2. PET data acquisition and reconstruction

The study population consisted of nine women in the early stage of dementia of Alzheimer's type. Their age ranged from 68 to 81 years (mean ± S.D. = 75.44 ± 5.0). The nine subjects were drawn randomly from a large pool of DAT patients participating in a study focusing on the neurofunctional effects of donepezil, a cholinesterase inhibitor, which is a medication used in the treatment of mild to moderate dementia of Alzheimer's type. This study was approved by the ethical committee of Geneva University Hospital and the Swiss Federal radiation protection authorities. All patients gave their written informed consent for participation in the study protocol.

The method used in clinical routine in our department for attenuation correction is based on the acquisition of an additional pre-injection transmission scan (10 min) using ^{137}Cs single-photon sources. A thermoplastic face mask was used to limit head motion and for accurate repositioning of patients for the emission scan as they are removed from the bed following the TX scan. PET data acquisition (25 min) started 30 min after intravenous injection of approximately 222 MBq of ^{18}F-[FDG] on the ECAT ART continuously rotating partial-ring positron tomograph (Siemens/CTI, Knoxville, TN) operated in fully 3D mode. This scanner is capable of acquiring both pre- and post-injection transmission scans. The advantages and drawbacks of each technique are well understood, the former being preferred owing to the absence of contamination of transmission images by emission photons, which can lead to gross underestimation of tissue attenuation [8].

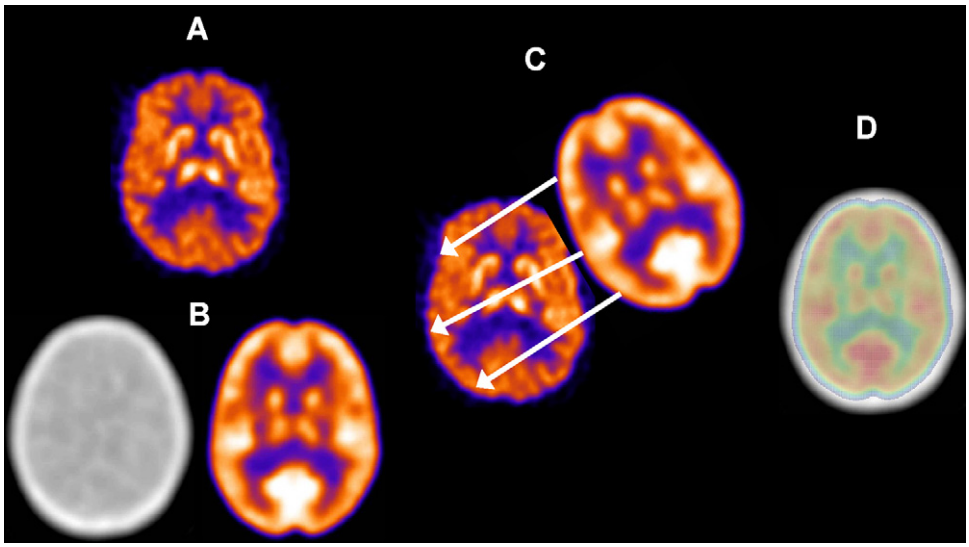

Fig. 1. Illustration of the principle of atlas-guided derivation of the attenuation map. (A) Preliminary PET reconstruction obtained using calculated attenuation correction. (B) ^{18}F-[FDG] emission and transmission templates used in this study. (C) Emission template is spatially normalized to preliminary PET reconstruction. (D) Application of same transformation to transmission template.

Images were reconstructed using analytic 3DRP reprojection algorithm [23] with a maximum acceptance angle corresponding to 17 rings and a span of 7. The default parameters used in clinical routine were applied (Ramp filter, cut-off frequency 0.35 cycles/pixel). The reconstructed images consist of 47 slices with 128×128 resolution and a voxel size set to $1.72\,\text{mm} \times 1.72\,\text{mm} \times 3.4\,\text{mm}$.

Scatter correction was performed using a model-based scatter correction algorithm which combines both the emission scan and attenuation map together with the physics of Compton scattering to estimate the scatter distribution [24]. The atlas-guided attenuation correction matrix is calculated by forward projection at appropriate angles of the resulting attenuation map. The generated attenuation correction factors are then used to correct the emission data. Therefore, the atlas-guided attenuation map served for both scatter and attenuation correction purposes.

2.3. Quantitative image analysis using BRASS

The images reconstructed with measured attenuation correction served as gold standard for assessment of the newly developed atlas-guided attenuation compensation. Reconstructed PET images using both attenuation correction methods were analysed using the *BRASS* commercial automated functional brain analysis software (Hermes *BRASS* software, Nuclear Diagnostics AB, Sweden). Briefly, *BRASS* fits and compares patient images to 3D reference templates created from images of healthy subjects. The transmission and atlas-guided reconstructed PET images were registered individually to the BRASS template for quantitative analysis. The ^{18}F-[FDG] template used in this work was built by averaging 12 PET images of normal subjects acquired on an ECAT EXACT HR^{+} PET scanner (Siemens/CTI, Knoxville, TN) in a fasting state with eyes open, ears plugged, and in a moderately lit environment. Fig. 2 illustrates transverse, coronal and sagittal views of the 3D anatomically standardised brain template and the region map consisting of a total of 63 regions defined on this template for automated VOI quantification [20]. The cost or optimization function used during automatic fitting to determine the similarity of the coregistered image to the template is based on *normalized mutual information* criterion which is similar to *mutual information* but is usually more robust and efficient in finding the correct fitting transform. The algorithmic implementation is based upon work by Studholme et al. [25]. Testing indicated that this was a better method than count difference or robust least squares, particularly when lesions are present in the brain study [20]. A comparison of some of these methods can be found elsewhere [26].

The correlation between mean activity concentration estimates obtained when using the two attenuation correction methods was checked on a VOI by VOI basis and using pooled VOI analysis. The means, standard errors and standard deviations of activity concentration estimates from clinical PET images reconstructed using both protocols were compared. The relative difference was used as a figure of merit for comparative assessment both within subject and as group consisting of a homogenous population. It is defined as:

$$\text{percent difference} = \frac{\text{VOI(Atlas-guided)} - \text{VOI(TX-guided)}}{\text{VOI(TX-guided)}} \times 100\%$$

Statistical analysis was performed VOI by VOI using repeated ANOVA to assess the significance of the differences between mean activity concentration estimates in patient studies when using the atlas-guided as compared to the transmission-guided reconstructions (significant P value <0.05). It should be noted that failure to prove statistically significant differences is not sufficient to confirm that the results are statistically identical.

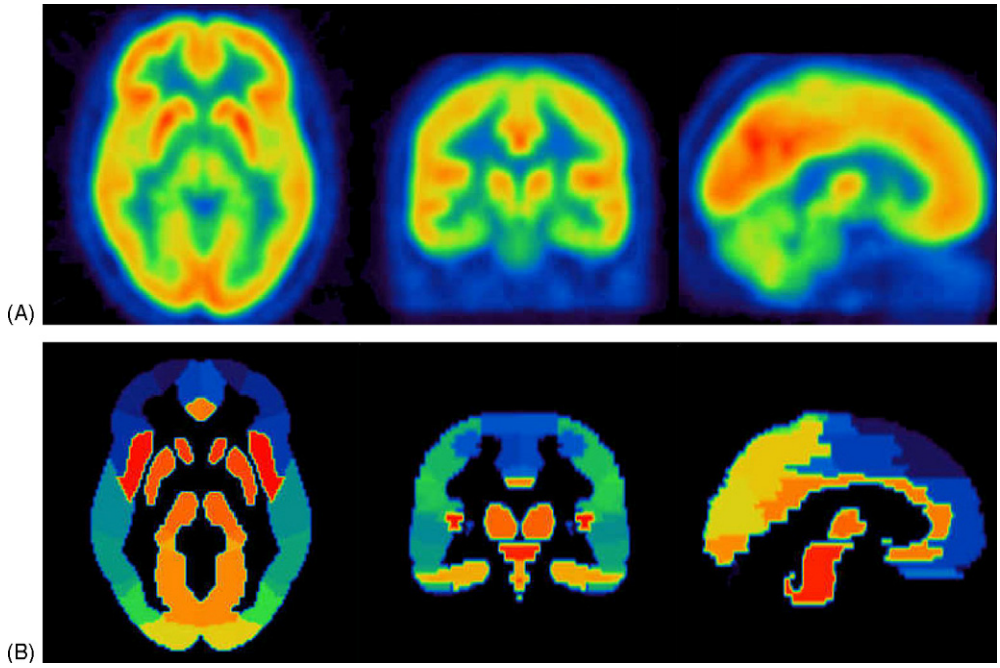

Fig. 2. Transverse, coronal and sagittal views (left to right) of the 3D anatomically standardized brain template (A) and the region map (B) consisting of 63 VOI regions in total defined on this template for automated VOI quantification (Hermes *BRASS* software, Nuclear Diagnostics AB, Sweden).

3. Results

Fig. 3 shows an example of original patient's PET images and the ^{18}F-[FDG] template in stereotactic coordinates together with the result of normalizing the template to these images. Note that the template matches quite well the patient's PET data. Typical patient brain non-uniform attenuation maps and corresponding PET images acquired on the ECAT ART camera and reconstructed with measured transmission as well as atlas-guided attenuation correction are shown in Fig. 4. The qualitative subjective assessment performed by expert physicians showed no significant visual differences between atlas-guided and transmission-based reconstruction methods [18]. Fig. 5 illustrates the means, standard errors as well as standard deviations of the relative differences between the two correction methods resulting from the quantitative analysis for the 63 VOIs, for each of the nine patients studied. The maximum difference within subject is less than 8%. Fig. 6 shows a linear regression plot illustrating correlation between the two attenuation correction algorithms for both a single patient and grouped analysis comprising the nine patients involved in the study. The line connecting the data points represents the result of a linear regression analysis. There is a very good correlation ($R^2 = 0.91$) between the atlas-guided and measured transmission-guided attenuation correction techniques and the regression line agreed well with the line of identity (slope = 0.96) for the grouped analysis. A slight dispersion of data points around the regression line can be observed and the general trend as shown by the regression line is that the coefficients of variations are similar. However, atlas-guided attenuation correction leads to higher overall estimates than measured attenuation correction. This would appear to result from a difference between the attenuation coefficient values in both methods and thus the attenuation correction factors applied. According to these results, the attenuation coefficients derived from the template obtained by positron-emitting ^{68}Ga/^{68}Ge rod sources appear to be slightly higher overall than estimates obtained from actual measured data using single-photon ^{137}Cs point sources. Moreover, our analysis suggests that the intercept in the regression line is significantly different from zero. Ideally, it would have been desirable to generate a new ^{137}Cs-based TX atlas on the same PET scanner used to assess the performance of the proposed method. However, restrictions imposed by ethical committees and difficulties of recruitment of healthy volunteers complicated the procedure.

The statistical comparison between activity concentration estimates when using the two attenuation correction techniques is summarized in Table 1. Correlation for all VOIs and all patients was found to be high. The percent differences between the two attenuation correction techniques are minor and no proof of statistically significant differences ("the two distributions are not the same") could be verified for all regions. Fig. 7 shows the relative difference between absolute activity concentration estimates for clinical brain 3D reconstructions using attenuation correction guided by measured transmission and 3D reconstructions guided by standardized transmission template. It can be seen that the mean absolute relative difference between the two methods for all VOIs across the whole population (differences of the population means) is 2.3% whereas the maximum difference is less than 7%. These results seem to suggest a 10% anterior–posterior gradient for a grouped data analysis performed by grouping the VOIs into regions by spatial location (i.e., medial/lateral, anterior/posterior, superior/inferior).

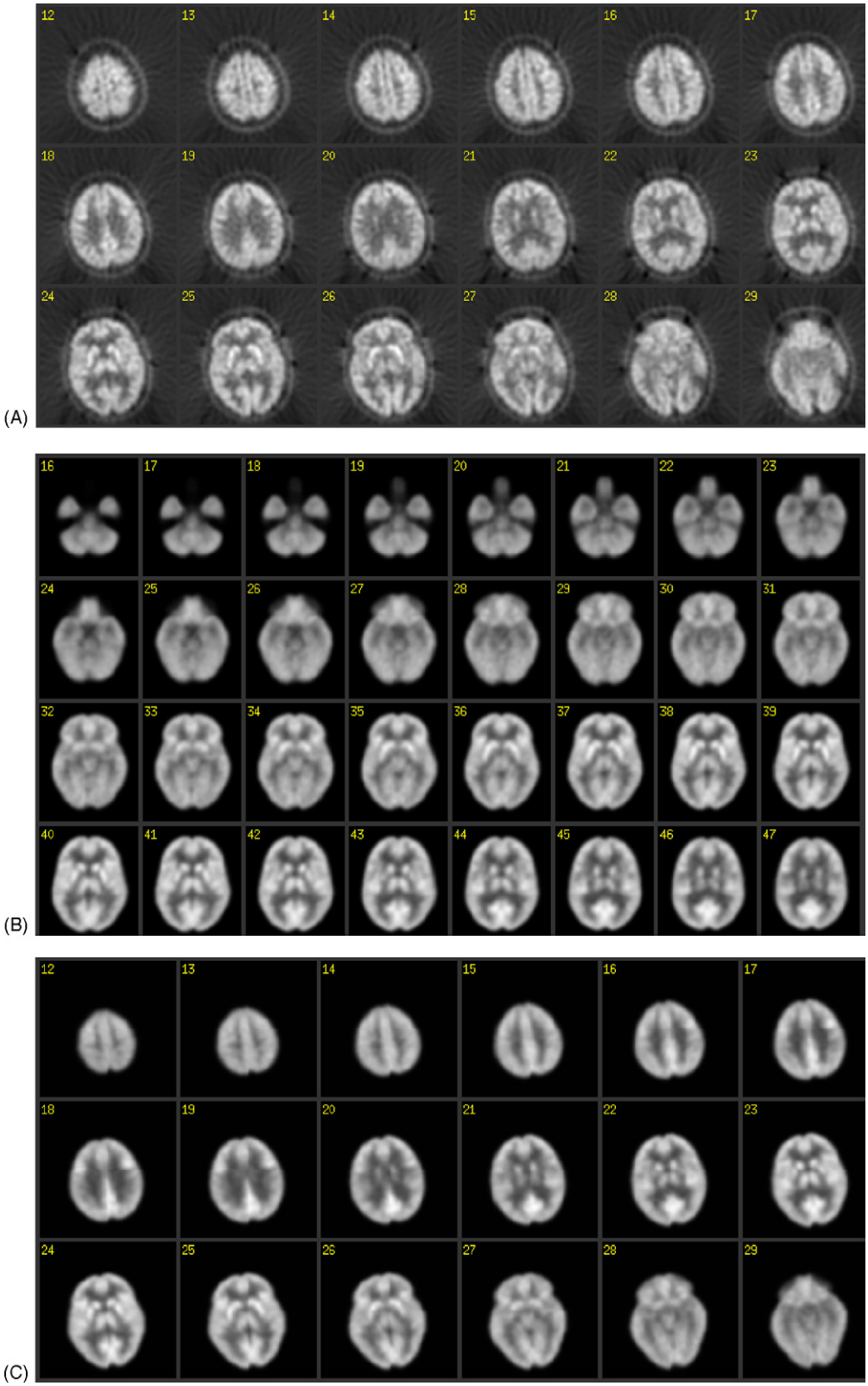

Fig. 3. Illustration of the accuracy of the spatial normalization procedure showing the preliminary reconstructions of ^{18}F-[FDG] patient PET images (A), the ^{18}F-[FDG] template in stereotactic space (B) and the resulting images of the emission template normalized to patient's PET images (C).

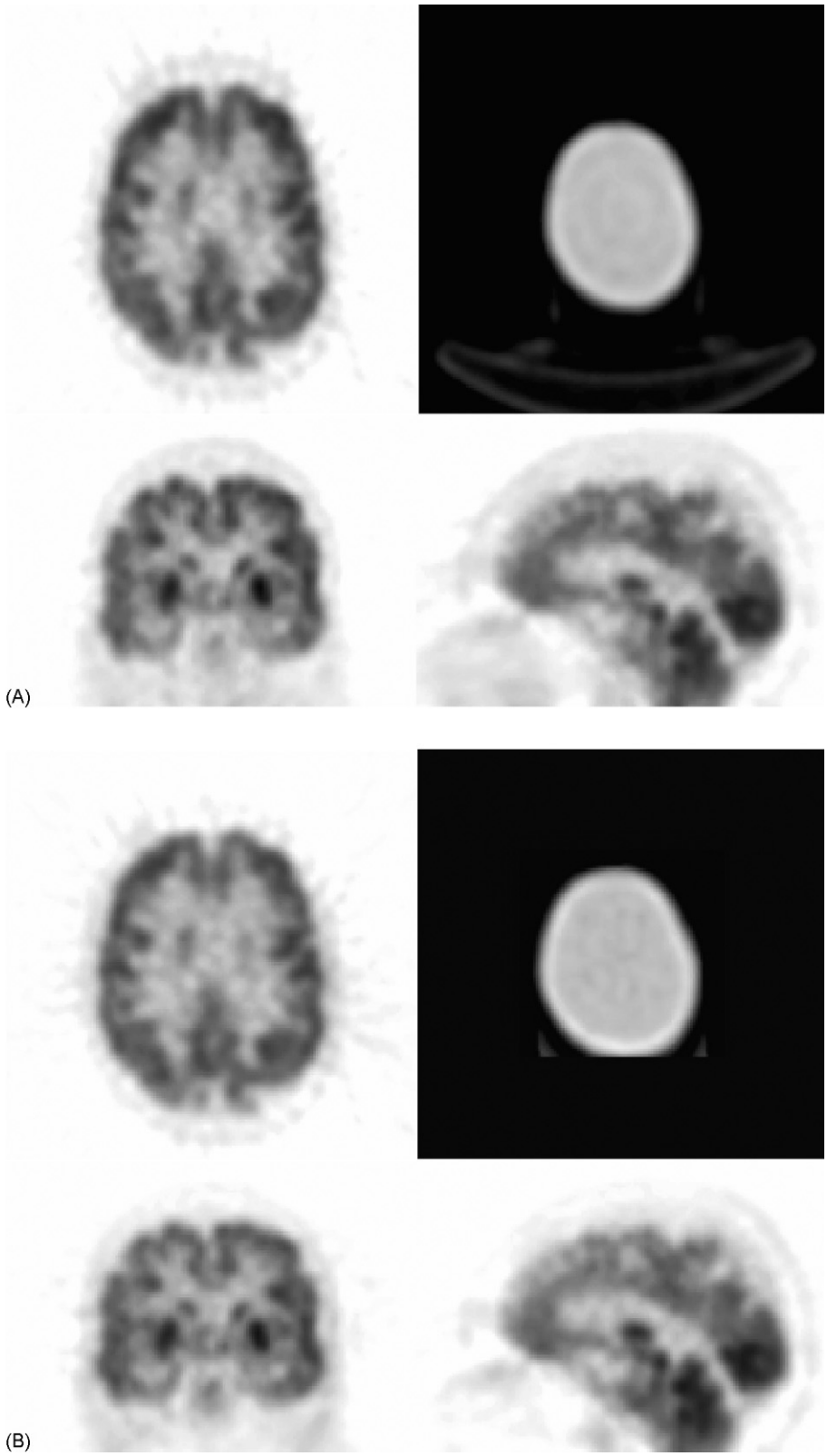

Fig. 4. Filtered backprojection reconstructions of clinical 3D brain PET images presented in different planes together with a corresponding slice of the attenuation map comparing measured (A) and atlas-guided (B) attenuation correction techniques.

Table 1
Summary of statistical assessment using repeated ANOVA analysis for comparing activity concentration estimates obtained from clinical brain PET reconstructions guided by measured transmission with atlas-guided reconstructions

Volume of interest	ANOVA significance	Paired sample correlation	Paired sample significance
R Cerebellum	0.550	0.947	<0.001
L Cerebellum	0.529	0.948	<0.001
R G. frontalis superior	0.040	0.939	<0.001
L G. frontalis superior	0.034	0.966	<0.001
R G. frontalis medius	0.101	0.921	<0.001
L G. frontalis medius	0.020	0.974	<0.001
R G. frontalis inferior	0.746	0.918	<0.001
L G. frontalis inferior	0.427	0.975	<0.001
R G. front. sup. pars med.	0.134	0.957	<0.001
L G. front. sup. pars med.	0.132	0.973	<0.001
R G. precentralis	0.677	0.914	<0.001
L G. precentralis	0.588	0.961	<0.001
R Lobulus paracentralis	0.156	0.968	<0.001
L Lobulus paracentralis	0.393	0.962	<0.001
R G. rectus	0.676	0.890	<0.001
L G. rectus	0.521	0.933	<0.001
R G. orbitalis	0.822	0.890	<0.001
L G. orbitalis	0.920	0.964	<0.001
R G. temporalis superior	0.534	0.947	<0.001
L G. temporalis superior	0.195	0.968	<0.001
R G. temporalis medius	0.858	0.933	<0.001
L G. temporalis medius	0.360	0.963	<0.001
R G. temporalis inferior	0.883	0.906	<0.001
L G. temporalis inferior	0.190	0.965	<0.001
R G. postcentralis	0.568	0.918	<0.001
L G. postcentralis	0.275	0.965	<0.001
R Lobulus par. inf.	0.613	0.901	<0.001
L Lobulus par. inf.	0.799	0.973	<0.001
R G. supramarginalis	0.587	0.908	<0.001
L G. supramarginalis	0.724	0.968	<0.001
R G. angularis	0.746	0.915	<0.001
L G. angularis	0.924	0.962	<0.001
R Lobulus par. sup.	0.576	0.934	<0.001
L Lobulus par. sup.	0.363	0.957	<0.001
R G. occipitalis sup.	0.947	0.927	<0.001
L G. occipitalis sup.	0.488	0.953	<0.001
R G. occipitalis medius	0.712	0.908	<0.001
L G. occipitalis medius	0.251	0.961	<0.001
R G. occipitalis inf.	0.609	0.952	<0.001
L G. occipitalis inf.	0.418	0.969	<0.001
R Cuneus	0.636	0.944	<0.001
L Cuneus	0.471	0.960	<0.001
R Precuneus	0.719	0.943	<0.001
L Precuneus	0.878	0.956	<0.001
R Uncus	0.410	0.919	<0.001
L Uncus	0.873	0.938	<0.001
R Hippocampus	0.112	0.949	<0.001
L Hippocampus	0.161	0.963	<0.001
R G. occipitotemp. lat.	0.728	0.920	<0.001
L G. occipitotemp. lat.	0.124	0.968	<0.001
R G. occipitotemp. med.	0.473	0.941	<0.001
L G. occipitotemp. med.	0.249	0.956	<0.001
R G. cinguli	0.653	0.973	<0.001
L G. cinguli	0.630	0.978	<0.001
R Thalamus	0.071	0.956	<0.001
L Thalamus	0.046	0.971	<0.001
R Putamen	0.639	0.945	<0.001
L Putamen	0.478	0.971	<0.001
R Caput nuclei caudati	0.759	0.973	<0.001
L Caput nuclei caudati	0.079	0.990	<0.001
Brain stem	0.058	0.949	<0.001
R Insula	0.160	0.956	<0.001
L Insula	0.176	0.978	<0.001

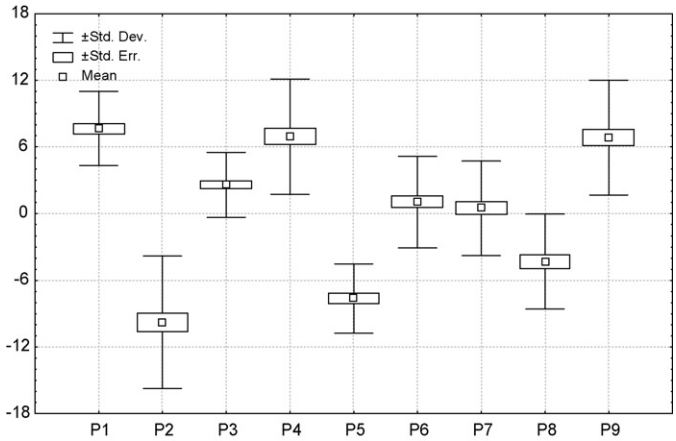

Fig. 5. Box & Whisker plots showing relative differences between reconstructions obtained by performing attenuation correction guided by measured transmission and normalized standardized template. Means, standard errors as well as standard deviations are calculated for each of the nine patients studied.

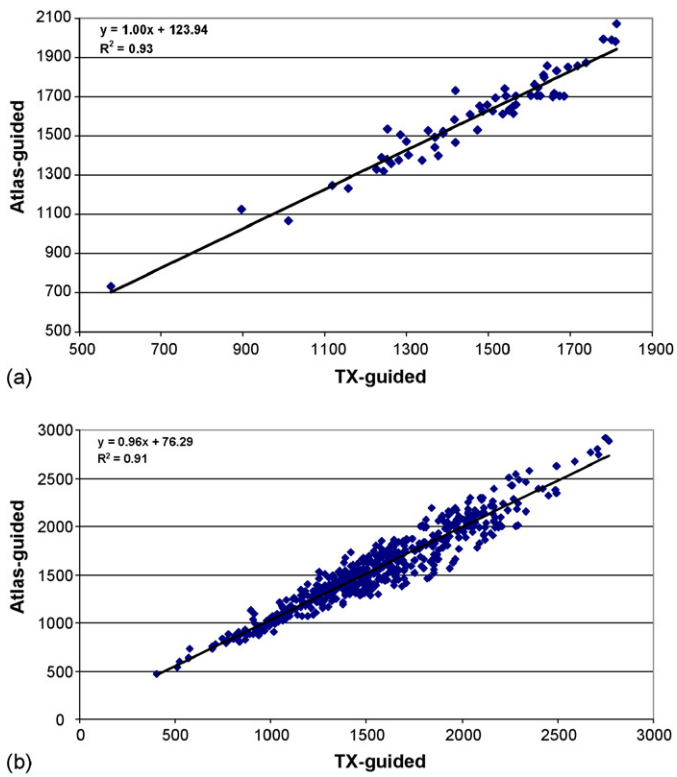

Fig. 6. Correlation plots between clinical 3D brain scans reconstructed using attenuation correction guided by measured transmission (abscissa) and 3D reconstructions guided by normalized standardized template (ordinate). Sixty-three data points for a single patient (a) and 567 data points representing mean values of the 63 VOIs resulting from the analysis of the nine patients studied are shown (b) together with best fit equations and correlation coefficients.

4. Discussion

Quantitative PET imaging of the brain continue to play an important role in the development of a common basis and language for neurology, psychiatry and psychology [2,3].

Despite the progress made in quantitative imaging, physical factors still degrade the actual image and thus the true activity obtained by PET measurements in functional brain imaging [6]. Therefore, it is not surprising that to improve brain mapping, it is imperative to investigate the impact of correction techniques for physical degradation factors such as attenuation, scatter and resolution loss or partial volume effect. Several methods have been devised to correct for attenuation in neurological PET studies that do no require an always noisy transmission scan [14–18]. It is worth emphasizing that despite the worthwhile research that has been performed in this area, there is no clear evidence that current commercial products allow applicability of these techniques in a clinical environment [7]. It should be highlighted that the efforts of the authors are focussed towards the development of quantitative imaging techniques for a "transmissionless" prototype based on a novel and innovative design of a high-resolution Compton-enhanced 3D brain PET camera. This concept leads to an image reconstruction, which is free of any parallax error and provides a uniform spatial and energy resolution over the whole sensitive volume [27,28]. In this regard, most brain dedicated PET scanners would benefit from the proposed technique. Likewise, the method is appealing as an alternative to CT-based attenuation correction on combined PET/CT scanners in the presence of artefacts of any nature (metals, contrast medium, . . ., etc.) and when radiation dose reduction to the subjects is sought (e.g., research protocols involving healthy volunteers). The technique might also be of interest for application on new dual-modality PET/MRI systems where the determination of the attenuation map from the MR image is still an open problem owing to the fact that the MR intensities are not directly related to the attenuation coefficients [16].

Like other image processing algorithms, the accuracy of PET attenuation correction algorithms must be validated and their limit tested before being applied to clinical or research data. This includes the assessment of the accuracy of the algorithms and their sensitivity towards methodological considerations. The accuracy of attenuation correction has been validated by simulated and experimental phantom studies, animal studies, biopsy samples taken after imaging was performed in addition to assessments involving clinical and healthy subject investigations [8]. It should be pointed out that the majority of proposed methods reported in the literature have been applied primarily to computer-simulated images and simplified experimental arrangements [7]. This has been extended more recently to objective assessment of image quality using receiver operating characteristics (ROC) analysis based on human or computer observers [29], evaluation of the influence of reconstruction techniques on tracer kinetic parameter estimation [30] and voxel-based analysis in functional brain imaging using statistical parametric mapping [10,31]. Some solutions to the problem of attenuation effects for instance are less suitable for routine applications in patients than they are in phantom simulations. The accuracy reached in phantom studies is unlikely to be reached in clinical investigations. The true clinical feasibility of these methods has yet to be fully investigated.

Evaluation and clinical validation of image correction and reconstruction algorithms is inherently difficult and sometimes unconvincing. There is a clear need for guidelines to evaluate quantitative techniques and other image processing issues in

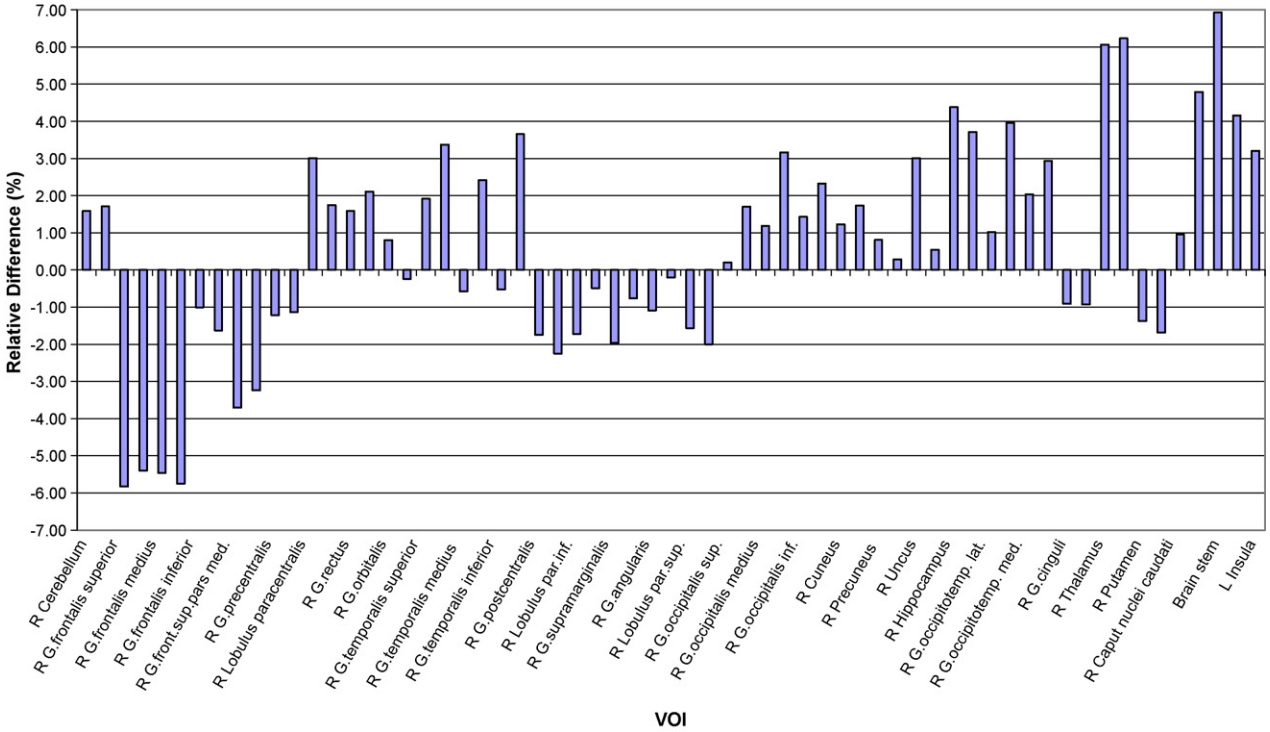

Fig. 7. Relative difference between absolute activity concentration estimates for clinical brain 3D reconstructions using attenuation correction guided by measured transmission and 3D reconstructions guided by normalized standardized template. For better visibility, only the right labels of the VOIs are shown except the insula where the left label is shown.

PET. Voxel-based or VOI-based analysis of PET algorithmic designs is intrinsically based on a large number of variables which all affect the final result to a greater or lesser extent. Acquisition and reconstruction options rely on isotope, acquisition time/injected activity, randoms, scatter and attenuation correction, reconstruction algorithm, pre- and/or post-filtering, . . ., etc. Subsequent analysis is done after (intra-individual) coregistration, anatomical standardization (spatial normalization) and smoothing. Therefore, it is clear that a multi-parameter optimization procedure is necessary to determine the optimal conditions for measuring defects or activations [32]. The clinical relevance of small but systematic differences (<8%) between the two attenuation correction methods is hard to predict and will depend on the diagnostic paradigm followed by clinicians to interpret brain PET data. Current procedures for interpreting clinical data in many PET facilities are still based on mere visual assessment. It has been shown that different attenuation correction techniques have little effect on subjective visual interpretation of brain PET images [17]. An in-depth discussion of relevant issues including the effect of abnormal anatomy and/or uptake in patients as well as the relevance of building tracer-specific templates especially for PET radioligands to allow application of the proposed algorithm for children and other tracers are given in [18]. For the former, the use of cost-function masking to exclude abnormal anatomy or uptake is envisaged to avoid biasing the transformations computed by the normalization procedure.

Nowadays, manual ROI analyses are no longer of much clinical interest since a long time is required to draw accurately the ROIs needed to cover an entire brain and the operator-dependent variability is large compared to inter-individual physiological variability. The artificial boundaries from the ROI or VOI region map and the relatively large search volumes constitute a known inherent disadvantage of VOI techniques in the sense that they imply a preconception about the topography of the functional deficits and that the size of the VOI imposes a spatially smoothing effect [33]. Smaller focal defects can be observed by the voxel-based techniques and a brain region can be reported as abnormal even when only part of the underlying VOI was hypoperfused (dilution effect). Additional tools for subject-to-group statistical comparisons should be available with automatic VOI-based analysis tools and these should take into account the special problems of correction for multiple comparisons [34,35]. However, if sufficient variance from the VOI measurements is included, the overall performance of automated stereotactic VOI-based analysis can be similar to that of the voxel-based analysis for the same discrimination task. In some studies, VOI-based analysis performed poorly at low false-positive fraction and was less tolerant to noise than the voxel-based analysis [36]. Another study found that under clinical conditions (in traumatic brain injury and cognitive impairment), classification of brain SPECT studies can greatly be aided by anatomic standardization techniques and that under the investigated circumstances, SPM was found to have a lower sensitivity than VOI or voxel-wise region-growing techniques, at low false-positive fractions, in contrast to the former study [37]. Given the considerations mentioned above, it was felt pertinent to complement the voxel-based analysis performed previously by the VOI-based analysis to provide a comprehensive assessment of the potential of the

proposed attenuation correction technique. Among the commercial packages, *BRASS* is specifically oriented towards routine clinical brain SPECT and PET applications, and allows voxel-wise comparison of individual studies by means of statistical intensity differences, compared to a mean and standard deviation image from a control group, based upon region-growing of deviating voxels.

5. Conclusion

A recently developed new atlas-guided non-uniform attenuation correction method for 3D brain PET imaging was assessed quantitatively using clinical studies and automated functional brain analysis software as an adjunct to the voxel-based analysis performed previously. The algorithm is unsupervised and shows a comparable image quality with significant reduction in overall patient scanning time duration and radiation absorbed dose. These encouraging results provide further confidence in the adequacy of the proposed method demonstrating its performance particularly for diagnostic applications involving quantification.

Acknowledgement

This work was supported by the Swiss National Science Foundation under grant SNSF 3152A0-102143.

References

[1] Gilman S. Imaging the brain. New Engl J Med 1998;338:812–20.
[2] Herholz K, Heiss WD. Positron emission tomography in clinical neurology. Mol Imaging Biol 2004;6:239–69.
[3] Costa DC, Pilowsky LS, Ell PJ. Nuclear medicine in neurology and psychiatry. Lancet 1999;354:1107–11.
[4] Zaidi H, Montandon M-L. The new challenges of brain PET imaging technology. Curr Med Imaging Rev 2006;2:3–13.
[5] Van Laere K, Zaidi H. Quantitative analysis in functional brain imaging. In: Zaidi H, editor. Quantitative analysis in nuclear medicine imaging. New York: Springer; 2005. p. 435–70.
[6] Zaidi H, Sossi V. Correction for image degrading factors is essential for accurate quantification of brain function using PET. Med Phys 2004;31:423–6.
[7] Zaidi H, Hasegawa BH. Determination of the attenuation map in emission tomography. J Nucl Med 2003;44:291–315.
[8] Zaidi H, Montandon M-L, Meikle S. Strategies for attenuation compensation in neurological PET studies. Neuroimage 2007;34:518–41.
[9] Hooper PK, Meikle SR, Eberl S, Fulham MJ. Validation of postinjection transmission measurements for attenuation correction in neurological FDG-PET studies. J Nucl Med 1996;37:128–36.
[10] van den Heuvel OA, Boellaard R, Veltman DJ, Mesina C, Lammertsma AA. Attenuation correction of PET activation studies in the presence of task-related motion. Neuroimage 2003;19:1501–9.
[11] Ay MR, Zaidi H. Computed tomography-based attenuation correction in neurological positron emission tomography: evaluation of the effect of x-ray tube voltage on quantitative analysis. Nucl Med Commun 2006;27:339–46.
[12] Ay MR, Zaidi H. Assessment of errors caused by x-ray scatter and use of contrast medium when using CT-based attenuation correction in PET. Eur J Nucl Med Mol Imaging 2006;33:1301–13.
[13] Kamel EM, Burger C, Buck A, von Schulthess GK, Goerres GW. Impact of metallic dental implants on CT-based attenuation correction in a combined PET/CT scanner. Eur Radiol 2003;13:724–8.
[14] Siegel S, Dahlbom M. Implementation and evaluation of a calculated attenuation correction for PET. IEEE Trans Nucl Sci 1992;39:1117–21.
[15] Weinzapfel BT, Hutchins GD. Automated PET attenuation correction model for functional brain imaging. J Nucl Med 2001;42:483–91.
[16] Zaidi H, Montandon M-L, Slosman DO. Magnetic resonance imaging-guided attenuation and scatter corrections in three-dimensional brain positron emission tomography. Med Phys 2003;30:937–48.
[17] Zaidi H, Montandon M-L, Slosman DO. Attenuation compensation in cerebral 3D PET: effect of the attenuation map on absolute and relative quantitation. Eur J Nucl Med Mol Imaging 2004;31:52–63.
[18] Montandon M-L, Zaidi H. Atlas-guided non-uniform attenuation correction in cerebral 3D PET imaging. Neuroimage 2005;25:278–86.
[19] Friston K, Ashburner J, Heather J, Holmes A, Poline JB. Statistical Parametric Mapping (SPM2), The Wellcome Department of Cognitive Neurology, University College London, London. Available at www.fil.ion.ucl.ac.uk/spm, 2003.
[20] Slomka PJ, Radau P, Hurwitz GA, Dey D. Automated three-dimensional quantification of myocardial perfusion and brain SPECT. Comput Med Imaging Graph 2001;25:153–64.
[21] Gispert JD, Pascau J, Reig S, Martinez-Lázaro R, Molina V, Desco M. Influence of the normalization template on the outcome of statistical parametric mapping of PET scans. Neuroimage 2003;18:601–12.
[22] Zaidi H, Diaz-Gomez M, Boudraa AE, Slosman DO. Fuzzy clustering-based segmented attenuation correction in whole-body PET imaging. Phys Med Biol 2002;47:1143–60.
[23] Kinahan PE, Rogers JG. Analytic 3D image reconstruction using all detected events. IEEE Trans Nucl Sci 1989;36:964–8.
[24] Watson CC. New, faster, image-based scatter correction for 3D PET. IEEE Trans Nucl Sci 2000;47:1587–94.
[25] Studholme C, Hill DLG, Hawkes DJ. An overlap invariant entropy measure of 3D medical image alignment. Pattern Recogn 1999;32:71–86.
[26] Radau PE, Slomka PJ, Julin P, Svensson L, Wahlund LO. Evaluation of linear registration algorithms for brain SPECT and the errors due to hypoperfusion lesions. Med Phys 2001;28:1660–8.
[27] Braem A, Chamizo Llatas M, Chesi E, Correia JG, Garibaldi F, Joram C, et al. Feasibility of a novel design of high-resolution parallax-free Compton enhanced PET scanner dedicated to brain research. Phys Med Biol 2004;49:2547–62.
[28] Seguinot J, Braem A, Chesi E, Joram C, Mathot S, Weilhammer P, et al. Novel geometrical concept of high performance brain PET scanner: principle, design and performance estimates. Nuovo Cimento C 2006;29:429–63.
[29] Narayanan MV, King MA, Pretorius PH, Dahlberg ST, Spencer F, Simon E, et al. Human-observer receiver-operating-characteristic evaluation of attenuation, scatter, and resolution compensation strategies for (99m)Tc myocardial perfusion imaging. J Nucl Med 2003;44:1725–34.
[30] Boellaard R, van Lingen A, Lammertsma AA. Experimental and clinical evaluation of iterative reconstruction (OSEM) in dynamic PET: quantitative characteristics and effects on kinetic modeling. J Nucl Med 2001;42:808–17.
[31] Montandon M-L, Slosman DO, Zaidi H. Assessment of the impact of model-based scatter correction on 18F-[FDG] 3D brain PET in healthy subjects using statistical parametric mapping. Neuroimage 2003;20:1848–56.
[32] Links JM. Special issues in quantitation of brain receptors and related markers by emission computed tomography. Q J Nucl Med 1998;42:158–65.
[33] Acton PD, Friston KJ. Statistical parametric mapping in functional neuroimaging: beyond PET and fMRI activation studies. Eur J Nucl Med 1998;25:663–7.
[34] Signorini M, Paulesu E, Friston K, Perani D, Colleluori A, Lucignani G, et al. Rapid assessment of regional cerebral metabolic abnormalities in single subjects with quantitative and nonquantitative [^{18}F]FDG PET: a clinical validation of statistical parametric mapping. Neuroimage 1999;9:63–80.
[35] Weeks RA, Cunningham VJ, Piccini P, Waters S, Harding AE, Brooks DJ. 11C-diprenorphine binding in Huntington's disease: a comparison of region of interest analysis with statistical parametric mapping. J Cereb Blood Flow Metab 1997;17:943–9.
[36] Liow JS, Rehm K, Strother SC, Anderson JR, Morch N, Hansen LK, et al. Comparison of voxel- and volume-of-interest-based analyses in FDG PET scans of HIV positive and healthy individuals. J Nucl Med 2000;41:612–21.

[37] Van Laere KJ, Warwick J, Versijpt J, Goethals I, Audenaert K, van Heerden B, et al. Analysis of clinical brain SPECT data based on anatomic standardization and reference to normal data: an ROC-based comparison of visual, semiquantitative, and voxel-based methods. J Nucl Med 2002;43: 458–69.

Marie-Louise Montandon received the MS degree in Cognitive Psychology and a PhD in Neuroscience from the universities of Geneva and Lausanne within the lemanic doctoral program in Neurosciences. She is an active member of the PET Instrumentation and Neuroimaging Laboratory (*PINLab*) of Geneva University Hospital. She is actively involved in developing imaging solutions for neuroscience research and clinical diagnosis. Her research centres on the development of improved methods for quantification of functional three-dimensional brain PET images using sophisticated image reconstruction and statistical analysis tools. She is recipient of many awards and distinctions among which the 2005 best PhD thesis award given by the Medical School of Geneva University and the Research Grant for the Advancement of Women 2004 given by the Advisory Board for the Advancement of Women, National Center of Competence in Research CO-ME (Computer Aided and Image Guided Medical Interventions).

Habib Zaidi is head of the PET Instrumentation & Neuroimaging Laboratory at Geneva University Hospital. He received a PhD and habilitation (Privat-docent) both in medical physics from Geneva University and is now actively involved in developing imaging solutions for cutting-edge interdisciplinary biomedical research and clinical diagnosis in addition to lecturing undergraduate and postgraduate courses on medical physics and medical imaging. He serves as associate editor for *Medical Physics*, the *International Journal of Biomedical Imaging* and the *International Journal of Tomography & Statistics* and is a member of the editorial board of *Computer Methods and Programs in Biomedicine*. He is regional Editor for Electronic Medical Physics News, a publication of the International Organization for Medical Physics (IOMP), and scientific reviewer for leading journals in medical physics, nuclear medicine and scientific computing. He is a senior member of the IEEE and a Vice Chair of the professional relations committee of the IOMP in addition to being affiliated to several International medical physics and nuclear medicine organisations. He is involved in the evaluation of research proposals for European and International granting organisations and participates in the organisation of international symposia and top conferences as member of scientific committees. He is a recipient of many awards and distinctions among which the prestigious 2003 Young Investigator Medical Imaging Science Award given by the Nuclear Medical and Imaging Sciences Technical Committee of the IEEE and the 2004 Mark Tetalman Memorial Award given by the Society of Nuclear Medicine. Dr. Zaidi has been an invited speaker of many keynote lectures at an International level, has authored over 130 publications, including peer-reviewed journal articles, conference proceedings and book chapters and is the editor of two textbooks on therapeutic applications of Monte Carlo calculations in nuclear medicine and quantitative analysis in nuclear medicine imaging.